Mo AND W DEPLETIONS IN CAI'S IN CARBONACEOUS CHONDRITES: A THEORETICAL STUDY OF THE EFFECTS OF NEBULAR TOTAL PRESSURE

Bruce Fegley, Jr. and Derrick Kong, Department of Earth, Atmospheric, and Planetary Sciences, Massachusetts Institute of Technology, Cambridge, MA 02139 USA

Introduction. It is well known that in many Ca, Al-rich inclusions (CAI's) in carbonaceous chondrites the refractory metals ($W, Re, Os, Ir, Mo, Ru, Pt$) display abundance patterns related to their volatility with the more refractory metals such as Re and Os being more enriched (relative to CI chondrite abundances) than less refractory metals such as Ru and Pt. However, as noted by Fegley and Palme (1), Mo and W do not always fit into this pattern because they are commonly more depleted than expected from their relative volatilities. For example, neutron activation analytical data from the Max-Planck Institut für Chemie, Mainz, FRG show that 22 out of 30 samples ($\sim$ 73%) display Mo depletions while 8 out of 30 samples ($\sim$ 27%) display W depletions (2). These depletions are not a vapor pressure effect because W is the most refractory of these 7 metals and Mo has a vapor pressure very similar to that of Ir. Instead, the Mo and W depletions are the result of an interplay between the vapor pressures of Mo and W and the tendency of these two metals to be oxidized in solar nebula gas. Fegley and Palme (1) discussed these (and other) factors in detail and proposed that the Mo and W depletions resulted from high temperature oxidation in the solar nebula. In particular, they found that at an assumed nebular total pressure of 10^{-3} bars oxygen fugacities 10^3 to 10^4 times greater than the fO_2 of solar composition gas were required for their calculations to reproduce the observed depletion patterns. However, they did not study the effects of variations in the nebular total pressure on their conclusions. This abstract presents the preliminary results of such a study.

Calculations. A revised version of the METKON code described by Fegley and Palme (1) was used in the calculations. Thermodynamic data for Mo and W oxide gases were taken from the new 3rd edition JANAF Tables (3). The CAI's included in this study are listed in Table 1, six of these display Mo depletions while two of these (Leo-1 Big Metal Grain, Allende TE) display Mo and W depletions. The electron microprobe analyses of Os-rich metal from the Ornans RNZ inclusion do not include W; however, the bulk sample displays a W depletion (4).

Results. Table 2 displays the results of our calculations at assumed nebular total pressures ranging from 10^{-1} to 10^{-9} bars. Figure 1 displays four comparisons of observed and calculated refractory metal patterns for CAI's with Mo depletions. Several important points are illustrated by these results. First, elevated H_2O/H_2 ratios (i.e., elevated over the solar value of $\sim 5 \times 10^{-4}$) are required to reproduce the observed Mo and W depletions over the entire pressure range studied. The corresponding oxygen fugacities (fO_2) and the difference between these values and the solar gas oxygen fugacity at the same temperature and pressure are also listed in Table 2. The relationship between H_2O/H_2 ratio and fO_2 is given by the equation

$$\log_{10} fO_2 = 2\log_{10}(H_2O/H_2) + 5.59 - 25,598/T \tag{1}$$

taken from Rubin et al. (5) and the $\Delta \log_{10} fO_2$ is defined by the equation

$$\Delta \log_{10}(fO_2) = \log_{10}(fO_2)\text{oxidizing} - \log_{10}(fO_2)\text{solar}. \tag{2}$$

Second, the H_2O/H_2 ratios required to match the observed Mo and W depletions decrease as the assumed total pressure decreases. In other words, slightly less oxidizing conditions are required at lower total pressures. However, even at an assumed nebular total pressure of 10^{-9} bars, the required fO_2 values are $\sim 10^2$ to 10^4 times greater than for solar gas. Third, at a constant total pressure (e.g., 10^{-3} bars), the calculated temperature and H_2O/H_2 values for the 9 inclusions studied generally fall within restricted ranges.

Summary. Calculated fits to the observed Mo and W depletions in CAI's always require elevated H_2O/H_2 ratios (i.e., elevated oxygen fugacities) relative to solar gas over a wide range of assumed nebular total pressures (10^{-1} to 10^{-9} bars). Lower nebular total pressures, which are predicted by recent solar nebular models (6), require less oxidizing conditions than higher nebular total pressures. However, even at very low pressures (10^{-9} bars) oxygen fugacities $\sim 10^2$ to 10^4 times greater than for solar gas are required.

Acknowledgments. This work was supported by NASA Grant NAG9-108 from the Planetary Materials and Geochemistry Program to MIT. D. K. was also supported by the MIT UROP Program. We thank H. Palme and B. Spettel for providing us with their unpublished neutron activation analyses of CAI's.

References. B. Fegley, Jr. and H. Palme 1985 *EPSL*, **72**, 311-326; (2) B. Fegley, Jr. and R. G. Prinn, 1988, Int'l. Geol. Congress abstract, (3) M. W. Chase, Jr. et al., 1985. *JANAF Thermochemical Tables*, 3rd ed.; (4) H. Palme et al. 1982 *EPSL*, **61**, 1-12; (5) A. E. Rubin, B. Fegley, Jr. and R. Brett, 1988 in Meteorites and the Early Solar System, ed. J. F. Kerridge and M. S. Matthews, Univ. of Arizona Press, Tucson, pp. 488-511; (6) A. P. Boss, 1988, *Science*, **241**, 565-567.

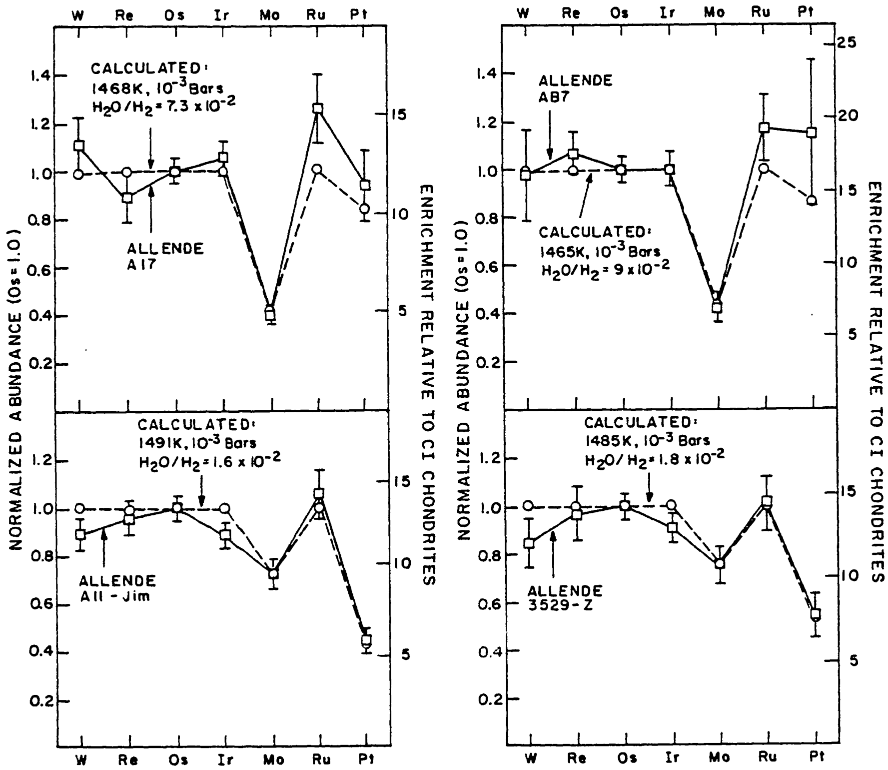

Table 1. Analytical Data for Refractory Metals in Selected *Ca, Al*-rich Inclusions and Calculated Patterns at 10^{-3} Bars Total Nebular Pressure

	CI Normalized Abundance (Os = 1.0)							Os
Sample	W	Re	Os	Ir	Mo	Ru	Pt	(ppm)
Allende AB7								
observed	0.98	1.07	1.00	1.00	0.42	1.17	1.15	8.22
calculated	0.99	1.00	1.00	1.00	0.44	1.00	0.91	
Allende A17								
observed	1.11	0.89	1.00	1.05	0.40	1.26	0.94	6.1
calculated	0.99	1.00	1.00	1.00	0.41	1.00	0.84	
Allende 3529-Z								
observed	0.85	0.97	1.00	0.91	0.75	1.01	0.54	7.1
calculated	1.00	1.00	1.00	1.00	0.76	1.00	0.53	
Allende All-Jim								
observed	0.89	0.96	1.00	0.89	0.73	1.06	0.45	6.46
calculated	1.00	1.00	1.00	1.00	0.73	1.00	0.43	
Efremovka EF62								
observed	0.86	0.86	1.00	0.89	0.62	1.01	0.66	9.91
calculated	1.00	1.00	1.00	1.00	0.60	1.00	0.70	
Allende AM1								
observed	0.87	1.04	1.00	0.92	0.71	0.96	0.64	17.7
calculated	1.00	1.00	1.00	1.00	0.70	1.00	0.61	
Lee-1 Big Metal Grain								
observed	0.50	1.16	1.00	0.95	0.028	0.36	0.080	5,000
calculated	0.83	1.00	1.00	0.86	0.015	0.52	0.004	
Allende TE								
observed	0.18	0.62	1.00	0.91	<0.06	0.82	<0.14	7.2
calculated	0.24	1.00	1.00	1.00	0.004	0.96	0.11	
Ornans RNZ								
observed	—	1.23	1.00	0.21	0.0012	0.15	—	37.6%
calculated	0.096	1.00	1.00	0.71	6.7×10^{-4}	0.31	0.002	

Notes: Estimated analytical uncertainties are <5% for Ir, Re, Os; 5-10% for W, Ru; and 10-30% for Pt (Fegley and Palme 1985). The analytical data are from Fegley and Palme (1985), Palme et al. (1982), and private communications from N. Palme and B. Spettel.

Table 2. Calculated Conditions for Matching Observed Refractory Metal Patterns in Selected *Ca, Al*-rich Inclusions.

	Nebular Total Pressure (Bars)				
	10^{-1}	10^{-3}	10^{-5}	10^{-7}	10^{-9}
Allende AB7					
Temperature (K)	1698	1465	1291	1166	1075
H_2O/H_2	1.5×10^{-1}	9.0×10^{-2}	7.0×10^{-2}	4.2×10^{-2}	2.5×10^{-2}
$\log_{10}(fO_2)$	-11.06	-13.94	-16.56	-19.17	-21.51
$\Delta \log_{10}(fO_2)$	5.04	4.55	4.28	3.80	2.30
Allende A17					
Temperature (K)	1699	1468	1292	1166	1075
H_2O/H_2	1.5×10^{-1}	7.3×10^{-2}	7.0×10^{-2}	4.2×10^{-2}	2.5×10^{-2}
$\log_{10}(fO_2)$	-11.27	-14.09	-16.54	-19.17	-21.51
$\Delta \log_{10}(fO_2)$	4.81	4.38	4.28	3.80	2.30
Allende 3529-Z					
Temperature (K)	1702	1485	1320	1214	1112
H_2O/H_2	3.5×10^{-2}	1.8×10^{-2}	1.7×10^{-2}	1.0×10^{-2}	8.0×10^{-3}
$\log_{10}(fO_2)$	-12.28	-15.10	-17.34	-19.53	-21.70
$\Delta \log_{10}(fO_2)$	3.77	3.15	3.06	2.57	2.33
Allende All-Jim					
Temperature (K)	1707	1491	1340	1222	1127
H_2O/H_2	2.4×10^{-2}	1.6×10^{-2}	1.1×10^{-2}	8.0×10^{-3}	6.0×10^{-3}
$\log_{10}(fO_2)$	-12.56	-15.13	-17.43	-19.58	-21.63
$\Delta \log_{10}(fO_2)$	3.45	3.05	2.69	2.38	2.10
Efremovka EF62					
Temperature (K)	1701	1475	1320	1205	1111
H_2O/H_2	5.5×10^{-2}	3.7×10^{-2}	2.2×10^{-2}	1.5×10^{-2}	1.0×10^{-2}
$\log_{10}(fO_2)$	-11.90	-14.59	-17.12	-19.34	-21.52
$\Delta \log_{10}(fO_2)$	4.16	3.78	3.28	2.92	2.53
Allende AM1					
Temperature (K)	1702	1480	1320	1206	1112
H_2O/H_2	4.0×10^{-2}	2.5×10^{-2}	1.8×10^{-2}	1.2×10^{-2}	8.0×10^{-3}
$\log_{10}(fO_2)$	-12.16	-14.87	-17.29	-19.51	-21.70
$\Delta \log_{10}(fO_2)$	3.89	3.44	3.11	2.73	2.33
Lee-1 Big Metal Grain					
Temperature (K)	1740	1620	1490	1400	1230
H_2O/H_2	7.8×10^{-2}	2.0×10^{-2}	1.0×10^{-2}	5.0×10^{-3}	8.0×10^{-3}
$\log_{10}(fO_2)$	-11.25	-13.54	-15.55	-17.28	-19.44
$\Delta \log_{10}(fO_2)$	4.47	3.27	2.64	2.02	2.38
Allende TE					
Temperature (K)	1730	1540	1390	1260	1160
H_2O/H_2	2.0×10^{-1}	1.5×10^{-1}	1.0×10^{-1}	8.0×10^{-2}	6.0×10^{-2}
$\log_{10}(fO_2)$	-10.52	-12.74	-14.81	-16.94	-18.97
$\Delta \log_{10}(fO_2)$	5.29	4.89	4.62	4.39	4.11
Ornans RNZ					
Temperature (K)	1840	1640	1500	1380	1275
H_2O/H_2	9.0×10^{-2}	7.0×10^{-2}	3.0×10^{-2}	1.5×10^{-2}	9.0×10^{-3}
$\log_{10}(fO_2)$	-10.31	-12.26	-14.48	-16.59	-18.59
$\Delta \log_{10}(fO_2)$	4.61	4.36	3.60	2.97	2.50